Uniform and local corrosion characterization and modeling for long-term exposure of different rebars used for RC elements in the presence of chloride conditions

Deeparekha Narayanan [a], Yi Lu[a], Ayman Okeil[b] and Homero Castaneda[a]

a, Department of Materials Science and Engineering, Texas A&M University (TAMU), 400 Bizzell St, College Station, TX 77843.
b, Department of Civil and Environmental Engineering, Louisiana State University, 3230J Patrick F. Taylor Hall, Baton Rouge, LA 70803.

Abstract. In this work we will present the corrosion behavior of ASTM 615 (steel rebar), ASTM 767 (Steel rebar with hot dip galvanized zinc layer) and ASTM 1094 (steel rebar with continuously galvanized zinc layer) rebars upon long-term exposure in simulated concrete pore solution (SCPS) with 3.5 wt.% NaCl. The rebars corrode in the SPS to form corrosion products on the surface and the chloride in the solution is responsible for the localized attack causing pit formation. The corrosion behavior was monitored continuously by electrochemical methods such as open circuit potential (OCP) and electrochemical impedance spectroscopy (EIS). Upon long-term exposure, the surface rebar conditions were characterized assuming uniform corrosion of the rebar due to the aqueous environment. Also, the concentration of NaCl used is beyond the so-called threshold passive breakdown layer in the selected environment. Following different exposure times for the study of localized corrosion, the rebars were characterized for pits and studied the depth distribution of the pits via optical microscopy (OM) The local attack morphologies and a detailed characterization of the pit distribution was carried out by measuring the depths of the identified defects. By sectioning at various locations, a more holistic idea about the pit distribution in the rebar was obtained. From the experimental results we were able to develop a framework for the two different conditions of the rebars used in the RC elements in the presence of chlorides and ambient conditions.

Keywords: Local pitting attack, RC Modeling, corrosion assessment.

1 Introduction

Reinforced concrete structures are frequently exposed to aggressive/corrosive environments that can promote deterioration of their structural properties and shortening of their service life. Chloride-induced corrosion of reinforcing steel in concrete represents one of the most severe and common forms of reinforced concrete degradation. Diffusion and accumulation of chloride ions within the concrete matrix and at the metallic surface interface promote the breakdown of the passive film formed as a result of the high alkaline pH of concrete on the reinforcing steel, and the initiation of localized corrosion at the steel surface. This chloride-

induced corrosion process can cause reduction of the cross-sectional area of the reinforcing steel. Recently the assumption of the loss of capacity due to the homogeneous degradation has some pitfalls, the most important is the local attack in some sites of the metallic rebar. To prevent or mitigate this damage process, surface modification in terms of inorganic or organic coatings are proposed as a control corrosion action due to their claims of excellent corrosion protection before any metallic activation. These coatings prevent the ingress of the chloride ions to the metal surface; hence, slowing down the formation of corrosion products and subsequent failure. This work orientates the damage evolution due to the chloride environment producing metal or wall thickness loss due to electrochemical reaction. The damage is also local due to the heterogeneous conditions of the microstructure distribution on the steel samples. Different works have carried the characterization of the corrosion conditions without considering a local attack. Pitting is a form of corrosion where localized loss of material occurs as opposed to a uniform loss. It is considered to be a more dangerous form because it is harder to detect and predict. In this work, we will use pitting corrosion models available in the literature to study the reliability of reinforced concrete rebars with different surface conditions that extend the life of the materials.

Several researchers investigated pitting corrosion of steel reinforcement in concrete structures. For example, K. Tutti [1] and Gonzalez et al. [2] modeled pitting corrosion within chloride-contaminated structures. The maximum pit depth, P_{max}, was found to exceed the penetration calculated based on general corrosion, P_{av} M. G. Stewart [3]. However, there is a significant uncertainty associated with the ratio between these two values. Gonzalez et al. [2] findings show that the maximum ratio of maximum pit depth to penetration of general corrosion, R, varies from 4 to 8 in concrete specimens exposed to natural environments. These results are generally in agreement with K. Tutti [1] who suggested that the ratio usually falls within a range of 4 to 10. Darmawan and Stewart [4] suggested the distribution of maximum pit depths for prestressing wires is best represented by the Gumbel (Extreme Value-Type I) distribution, which has been widely used to characterize other pitting corrosion scenarios such as that in steel plates and pipes as well as prestressing strands. M. G. Stewart [3] agreed that it is, therefore, reasonable that the Gumbel distribution be appropriate for modeling maximum pit depths of reinforcing bars. In this work we will present the corrosion behavior of several rebars exposed in simulated concrete pore solution (SCPS) with 3.5 wt.% NaCl at room temperature. The rebars corrode in the SPS to form corrosion products on the surface and the chloride in the solution influences the localized attack causing pit formation. The corrosion rate was characterized continuously by electrochemical impedance spectroscopy (EIS) and deterministic analysis while the pitting was characterized by high resolution techniques.

2 Experimental Procedure

Four rebars were selected to carry out the study – ASTM A615 bare steel rebar, ASTM A767 hot-dip galvanized (HDG) rebar, and ASTM A1094 continuous galvanized rebar (CGR) which will be referred to henceforth as 615, 767, and 1094 respectively. The rebars

were coated with epoxy only exposing a length of 6 cm (exposure area=33.51 cm^2) were immersed in a SCPS whose concentration is given in Table 1. Open circuit potential (OCP) and electrochemical impedance spectroscopy (EIS) tests were carried out on the rebars using a 3-electrode configuration (shown in Fig. 1(a)). Three rebars of 615, 767 and 1094 have immersed long term for about 20 months with the results from the general corrosion testing reported for up to 30 days of immersion and for long-term exposure. Since triplicates of the rebars were immersed, they were removed one by one after fixed intervals and cleaned using techniques mentioned in ASTM G1–03. [5] The samples were then examined to identify colonies of pits whose distance from a fixed point on the rebars were measured. They were then sectioned at these locations and the cross sections were studied under an Olympus DXS 500 optical microscope to measure pit depths. This procedure is shown in Fig. 1(c) and provides a reasonable idea of the pit distribution in the rebar. This distribution was obtained only for long-term immersed samples of each rebar tested.

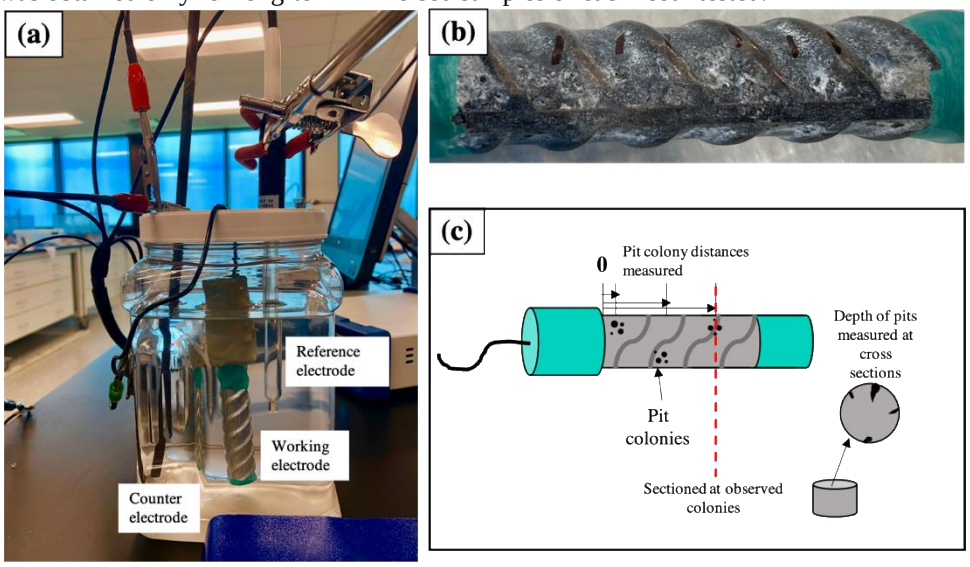

Fig. 1. (a) 3-electrode experimental set-up, (b)removed rebar showing markings of pit colonies and (c) schematic showing procedure employed to obtain pit distribution.

Table 1. Composition of pore solution and electrolyte used in the study.

KOH (M)	NaOH (M)	$Ca(OH)_2$ (M)	NaCl (wt%)
0.08	0.02	0.001	3.5

3 Results

The OCP, corrosion rate and charge transfer resistance calculations of the studied rebars are shown in Fig. 2. The sacrificial protection behavior of galvanized rebar samples is commonly studied by monitoring the OCP of the system. Metallic zinc exhibits highly negative OCP values of about -1.4 V vs. SCE when exposed to simulated concrete environments. For bare steel the corrosion degree is assessed based on the OCP values reported by Broomfield et al. [6] and is at a high risk of corrosion when the OCP values are more negative than -426 mV vs. SCE. It is evident that the bare steel is actively corroding after three days of immersion as seen in Fig. 2a due to the presence of chloride ions (higher concentration than the breakdown threshold) in the solution that induces the breakdown of the passive film and the initiation of corrosion.

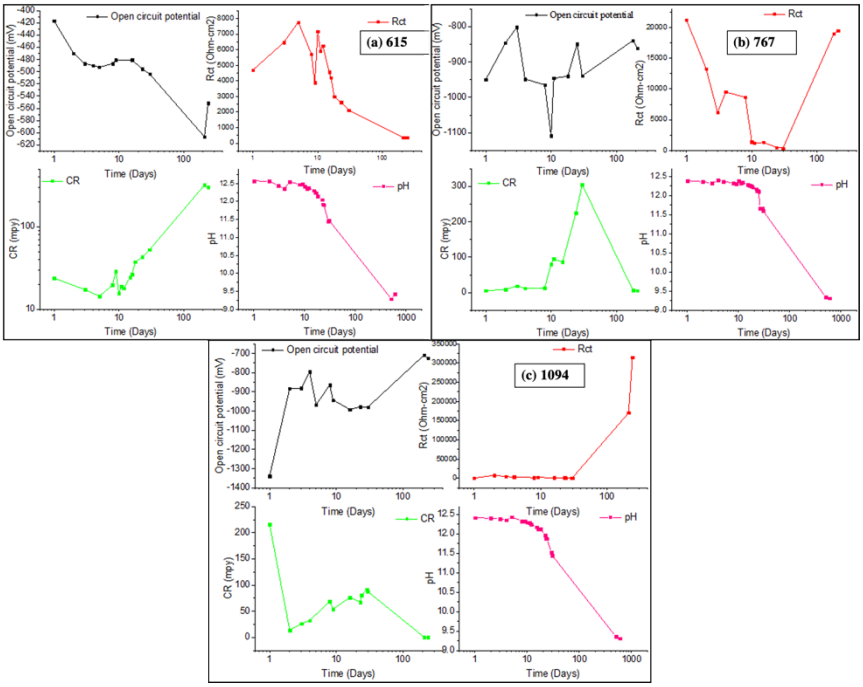

Fig. 2. Open circuit potential (vs Ag/AgCl), charge transfer resistance, corrosion rate plots of (a) 615, (b) 767 HDG, and (c) 1094 CGR rebar and their corresponding pH values in the saturated pore solution.

For the case of the galvanized rebar, we assessed the performance of these specimens according to the cathodic protection criterion. In this study, the OCP of the bare rebar in the

simulated concrete pore solution is about -500 mV vs. SCE as seen in Fig. 2**Fig. *5***. Therefore, we defined the cathodic protection limit as -600 mV vs. SCE following the 100-mV polarization development/decay. The OCP values of the galvanized rebars (767, 1094) were below the cathodic protection limit suggesting that during all exposure time (>400days), they were effective in providing sacrificial protection to the reinforcing steel. The pH magnitude was measured with time, the SCPS started with a pH magnitude of 12.5 and decreased with time, the pore solution became more acid due to the CO_2 exposure at room conditions, the ambient conditions influenced the pH following the first 10 days with a magnitude drop to 12. The first 30 days the pH included a magnitude of 11.5, the magnitude decrease to 9.4 when the solution was exposed to more than 400 days. The decrease follows a constant decay with time as illustrated in Fig. 2.

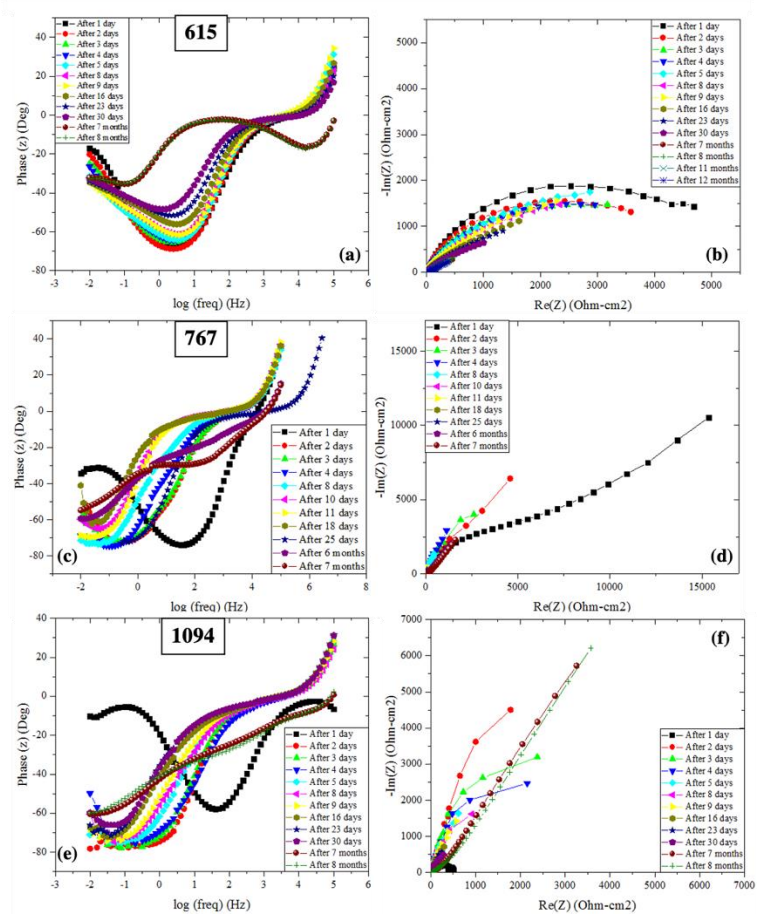

Fig. 3. Evolution of Bode plots and Nyquist plots of (a-c) 615, (d-f) 767 HDG, (g-i) 1094 CGR and (j-l) 9100 rebars in SCPS with time.

The evolution of the EIS (Nyquist and Bode representations) for the rebar specimens with time of immersion in the simulated concrete pore solution are displayed in Fig. 3. The Nyquist or complex representation of the bare steel (Fig. 3b) shows one capacitive loop that can be associated with the electrochemical activity at the steel/electrolyte interface. The arc gradually decreases with time suggesting a continuous degradation of the carbon steel substrate by the chloride ions for the 615 sample.

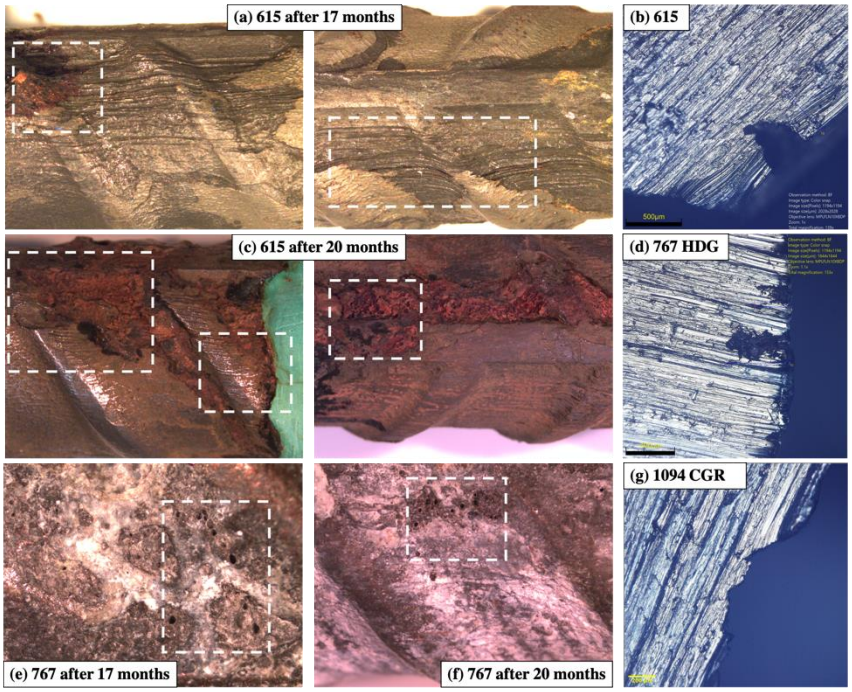

Fig. 4. Images showing pits of the surfaces of (a) 615 steel rebars after 17 months, (c) 615 after 20 months, (e) 767 after 17 months and (f) 767 after 20 months; Example images of pits observed along the cross sections of cut rebar imaged using an optical microscope are shown for (a) 615, (d) 767 and (g) 1094 rebars.

The EIS spectra evolution of the galvanized coatings systems show a similar trend between them. During the first day of immersion, the EIS signal shows one-time constant that can be related to charge transfer processes between the galvanized coating and the electrolyte solution. Early days of immersion, the phase angle plots show the presence of two-time constants, the time constant at high frequency can be associated with the charge transfer process whereas the one at lower frequencies can be related to the formation of zinc corrosion products on the coated rebar. The galvanized samples show an increased in impedance after few days of initial immersion, which is mainly attributed to the formation of zinc corrosion products that can provide an extra barrier protection against aggressive

species. However, at longer immersion time, there is a decrease in impedance, suggesting that the chloride ions attack the corrosion products and reactivate the galvanized layer. The results show different times of immersion, the evolution in impedance for longer times marks the mechanism where the corrosion products are formed and accumulate a thicker corrosion product. Fig. 4 shows the images of pits on the samples and some of pits observed on the edges of the cut sections. The pit colony distances and depths measured are listed in Table ***2*** and
Table ***3***. These results were used for the localized model developed.

Table 2. Pit colony distances measured in tested samples.

Colony #	615 (after 17 months, cm)	615 (after 20 months, cm)	767 (after 17 months, cm)	767 (after 20 months, cm)	1094 (after 17 months, cm)	1094 (after 20 months, cm)
1	0.1	0.6	0.9	0	1.8	0.5
2	0.9	1.5	1.8	1	2.6	1
3	2	2.5	2.5	2.2	3.3	2.6
4	2.8	4.4	3.5	3.5	4.2	4
5	3.9	5.2	4	4.3	5.5	5
6	4.6	5.6	4.6	5.6	-	5.5
7	5.4	-	5.2	-	-	5.6

Table 3. Pit depths measured on the cross sections of the samples.

615 (after 17 months, µm)	Expected colonies based on section location	767 (after 17 months, µm)	Expected colonies based on section location	1094 (after 17 months, µm)	Expected colonies based on section location
96.764	Colony 6	46.112	Colony 5	76.069	Colony 5
132.474		43.157		148.65	
91.871	Colony 5	459.116		202.18	
152.421		166.678		144.138	Colony 3
277.894		110.899	Colony 6	90.029	
290.858	Colony 3	31.782		216.776	Colony 2
145.615		118.226	Colony 4	89.794	
143.293		497.801	Colony 3	301.523	Colony 1
194.067		97.694		-	

363.33	Colony 4	523.939	Colony 1	-
151.111		279.04		-
328.33	Colonies 1 and 2	-		-
102.659		-		-
87.399		-		-
184.315		-		-
150.477		-		-
432.98		-		-
484.965		-		-

3.1 Framework for local attack

A popular approach in modeling pit depth using extreme value theory originates from A. Turnbull [7]. The ratio of maximum pit depth to average penetration from general corrosion, R, is treated as a random variable modeled by the Gumbel distribution using Eq. 1. This random variable is also referred to as the pitting factor.

$$F(R) = e^{-e^{-(R-\mu)/\alpha}} \tag{1}$$

where μ is the location parameter and α is the scale parameter, which characterizes the shape of the distribution; i.e., an indication of the dispersion of the data. M. G. Stewart [3] suggested that these parameters can be determined from the results of Gonzalez et al. [2]. For an 8-millimeter bar, R=4 and R=8 represent the 5th and 95th percentiles of the distribution, respectively. Accordingly, the mean and coefficient of variation are found to be 5.65 and 0.22, which translate into the parameters of the Gumbel distribution μ_0=5.08 and α_0=1.02. A. Turnbull [7] suggests that for a reinforcing bar with different dimensions, the Gumbel distribution parameters can be determined using Eqs. 2 and 3. Fig. 5a shows a plot of the PDF of R.

$$\mu = \mu_0 + \frac{1}{\alpha_0} ln\left(\frac{A}{A_0}\right) \tag{2}$$

$$\alpha = \alpha_0 \tag{3}$$

where, A is the surface area of the respective bar, and A_0 surface area of an 8mm diameter bar of 125 mm length.

After the statistical descriptors of the pitting factor random variable, R, the maximum pit depth along a reinforcing bar can be evaluated using Eq. 4.

$$P(T) = 0.0116 * i_{corr}(T) * R * T \quad (4)$$

This equation considers Faraday's law where a unit current density induces a uniform corrosion penetration of 11.6 micrometers per year [8]. A model to predict the loss of the cross-sectional area of a reinforcing bar due to pitting has been proposed by Val and Melchers [9]. The pit area, $A_{Pit}(T)$, can be estimated as a function of pitting depth.

Consequently, the residual steel area after pitting corrosion, $A_s(T)$, can be obtained using Eq. 5 for an initial nominal reinforcing bar diameter D_o.

$$A_s(T) = n\left(\frac{\pi D_0^2}{4} - A_{Pit}\right) \geq 0 \quad (5)$$

The flexural limit state function for the reliability analysis is built on fundamental reinforced concrete flexural analysis, where the nominal flexural strength, M_n, is estimated using Eq. 6 for rectangular sections with a width, b, an effective depth, d, concrete compressive strength, f_c', and steel yield stress, f_y. The depth of the equivalent compression stress block, a, can be found from equilibrium. It can be seen that the area of steel rebars directly affects the flexural resistance of reinforced concrete sections.

$$M_n = A_s * f_y * \left[d - \frac{a}{2}\right] \quad (6)$$

The limit state function for flexural strength represents the difference between the resistance, M_R and the demands due to external loads, M_Q. Substituting for all the aforementioned variable in the limit state function, the limit state function, $g(M)$, is given by Eq. 7 (Ghanooni-Bagha et al. [10]).

$$g(M) = \lambda_m M_n - M_Q = \lambda_m \left\{A_s(T) * f_y(T) * \left[d - K * \frac{A_s * f_y(T)}{b * f_c'}\right]\right\} - M_Q \quad (7)$$

where λ_m is a random variable representing flexural model uncertainty, $f_y(T)$ is the residual yielding steel strength of steel reinforcement (N/m^2) an accounting for stress concentrations due to pitting, the residual steel yield stress is computed using Eq. 8.

$$f_y(T) = \left(1 - \alpha * \frac{A_s - A_s(T)}{A_s}\right) * f_y \quad (8)$$

where α yield stress uncertainty coefficient and f_y initial yield stress of steel reinforcement (N/m^2). Using the First Order Reliability Method (FORM), the reliability index, β, can be determined for the limit state function over the design life of a reinforced concrete beam taking into account pitting corrosion as can be seen Fig. 5b. The resulting information can

be used as a tool for planning rehabilitation activities once a projected reliability threshold, β_{th}, is reached.

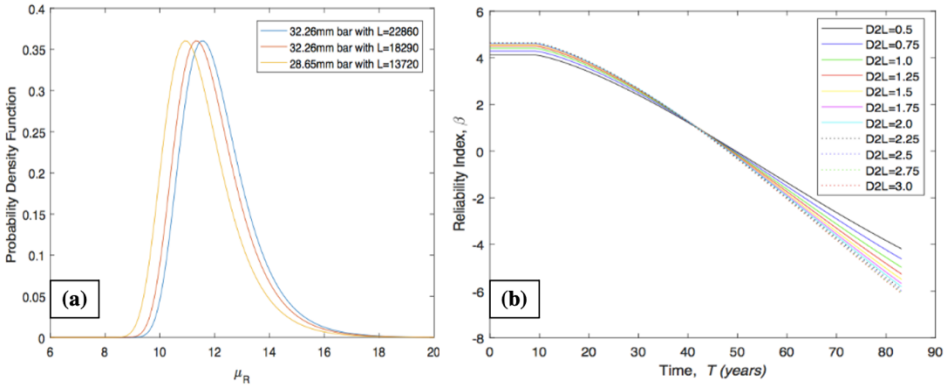

Fig. 5. Sample results: (a) PDF of R, (b) Reliability Index (β) vs. Time based on the local attack model.

4 Conclusions

The localized model is a more realistic approach for the reliability assessment, however the combination of both should be implemented, general corrosion and localized attach could be the next step for the reliability assessment. The preliminary framework is based on corrosion assessment by considering the damage evolution as the main threat.

Acknowledgments

The authors would like to acknowledge the funding support by the Tran-SET Project No.19STLSU10. The authors also would like to thank Dr. Yenny Cubides for the experimental results activities.

References

1. K. Tuutti, *Corrosion of Steel in Concrete*, Swedish Cement and Concrete Research Institute, Stockholm, 1982.
2. J.A. González, C. Andrade, C. Alonso and S. Feliu, *Comparison of rates of general corrosion and maximum pitting penetration on concrete embedded steel reinforcement*, Cem. Concr. Res. 25 (1995), pp. 257–264.
3. M.G. Stewart, *Spatial variability of pitting corrosion and its influence on structural fragility and reliability of RC beams in flexure*, Struct. Saf. 26 (2004), pp. 453–470.
4. M.S. Darmawan, *Spatial Variability of Pitting Corrosion and Its Effect on the Strength and*

Reliability of Prestressing Wires and Strands / M. Sigit Darmawan and Mark G. Stewart, Research report (University of Newcastle (N.S.W.); no. 246.05.2004.Centre for Infrastructure Performance and Reliability, University of Newcastle, Callaghan, N.S.W, 2004.

5. *ASTM G1-03(2017)e1, Standard Practice for Preparing, Cleaning, and Evaluating Corrosion Test Specimens*. ASTM International, West Conshohocken, PA, 2017.
6. J.P. Broomfield, *Corrosion of Steel in Concrete: Understanding, Investigation, and Repair*, London: E & FN Spon, 1997.
7. A. Turnbull, *Review of modelling of pit propagation kinetics*, Br. Corros. J. 28 (1993), pp. 297–308.
8. J. El Hassan, P. Bressolette, A. Chateauneuf and K. El Tawil, *Reliability-based assessment of the effect of climatic conditions on the corrosion of RC structures subject to chloride ingress*, Eng. Struct. 32 (2010), pp. 3279–3287.
9. D.V. Val and R.E. Melchers, *Reliability of deteriorating RC slab bridges*, J. Struct. Eng. 123 (1997), pp. 1638–1644.
10. M. Ghanooni-bagha, M.A. Shayanfar, O. Reza-Zadeh and M. Zabihi-Samani, *The effect of materials on the reliability of reinforced concrete beams in normal and intense corrosions*, Eksploat. I Niezawodn. Reliab. 19 (2017), pp. 393–402.